Journal of Cell Science 106, 685-692 (1993)
Printed in Great Britain © The Company of Biologists Limited 1993

Keratocyte networks visualised in the living cornea using vital dyes

C. Anthony Poole[1], Nigel H. Brookes[2] and Gillian M. Clover[2,*]

Departments of [1]Anatomy and [2]Surgery, School of Medicine, University of Auckland, Private Bag 92019, Auckland, New Zealand

*Author for correspondence at Ophthalmic Section, Department of Surgery

SUMMARY

Fluorescent viability probes have been used to visualise and investigate the viability, morphology and organisation of the keratocyte within the stroma of the intact living cornea. The live cell probe, calcien-AM, in combination with a dead cell probe, ethidium homodimer (Live/Dead Assay, Molecular Probes, U.S.A.) proved superior to earlier generation vital dyes such as fluorescein diacetate or 5,6-carboxyfluorescein diacetate, initially used in combination with ethidium bromide. The ubiquitous distribution of esterase enzymes that cleave calcien-AM within the keratocyte cytoplasm produced a high concentration of fluorescently active calcein throughout the cell, including fine cell processes. Epi-illuminated fluorescence microscopy on transparent corneal dissections subsequently revealed details of keratocyte microanatomy and three-dimensional network organisation in situ. Three morphologically discrete subpopulations of keratocytes were identified: two formed relatively small bands of cells, immediately subjacent to either Bowman's or Descemet's membranes, the third subpopulation constituting the majority of keratocytes typically located within the corneal stroma. The results indicate that calcein-AM is able to penetrate intact living cornea revealing cell viability, and it also has the capacity to 'trace' cellular elements and reveal fine structure within a dense connective tissue matrix.

Key words: cornea, keratocytes, viability dyes, calcein-AM, fluorescein diacetate, microanatomy, fluorescence microscopy

INTRODUCTION

This report demonstrates the use of fluorescent viability probes to investigate the organisation, morphology and viability of keratocytes in the living cornea. We introduce the use and unusual application of a combination of new generation fluoroprobes, Live-Dead Assay, which in this study has proved to be a particularly effective stain for enhancing the visibility of the diverse and intricate three-dimensional keratocyte network within the stroma of this transparent tissue.

The cornea forms the transparent anterior part of the continuous external coat of the eye globe and functions to transmit and refract light. It is bounded anteriorly by a multicellular epithelium to which the tear film adheres, and posteriorly by a single endothelial cell layer bathed by aqueous humour. Between these cellular layers is the stroma, a collagen-rich connective tissue comprising 90% of the total volume of the cornea. The principal stromal cell is the keratocyte (Maurice, 1984), a modified fibroblast derivative forming a flattened and attenuated cell with multiple cell processes. It is responsible for the development and maintenance of the extracellular matrix, the highly organised nature of which contributes to corneal transparency.

The keratocyte was first described by Toynbee in 1841, but detailed histological analysis was not performed until much later (Sverdlick, 1954; Scharenberg, 1955). Using silver impregnation, these workers demonstrated cells in the corneal stroma with large, flattened and eccentric nuclei, and a highly vacuolated cytoplasm. Although the cell borders were difficult to determine, cells lay between the collagen lamellæ, and seemed to contact each other by a syncytium of long cytoplasmic processes. Subsequently, these cell processes were shown to connect by a variety of specialised membrane junctions. Using ultrastructural techniques, Smith and co-workers (1969) found evidence of desmosomes, whereas Hogan and co-workers (1971) found tight junctions, both junctions being associated with structural support rather than intercellular communication. More recently, gap junctions have been identified at the point of contact between keratocyte processes (Ueda et al., 1987) and in isolated keratocytes cultured in three-dimensional collagen lattices (Assouline et al., 1992). Such junctions are known to provide metabolic contact between adjacent cells, and their presence in keratocytes implies transcellular communication.

The morphology of the keratocytes was subsequently examined by scanning electron microscopy (Nishida et al., 1988). Using proteolytic enzymes to extract the collagen lamellæ and physical dissection of the remaining structures, Nishida and co-workers confirmed the presence of an extensive network of cell processes. They suggested that the ker-

atocytes were arranged in this manner to maintain synchronised metabolic homeostasis of the corneal stroma.

Keratocyte metabolism has been studied in a number of biochemical, immunohistochemical and cell culture models. For example, it has been shown to synthesise and secrete collagen types I, III, V and VI (Birk et al., 1981, 1990; Cintron and Hong, 1988), the glycosaminoglycans hyaluronan, keratan sulphate, chondroitin 4-sulphate, chondroitin 6-sulphate, unsulphated chondroitin and heparan sulphate (Birk et al., 1981), and glycoproteins such as fibronectin, laminin and nidogen (Kohno et al., 1987; Schittny et al., 1988). The interaction between these extracellular matrix macromolecules and water, which makes up almost 78% of the stromal volume, determines the transparency and refractile properties of the cornea (Maurice, 1957), but it is not yet fully understood how the keratocytes are coordinated to achieve this function.

None of these methods allows direct visualisation of the keratocyte in the intact cornea. In this study we use fluorescent viability dyes to specifically examine the organisation, structure and vitality of keratocytes in the living cornea. Two families of fluorescent stains were evaluated that measure two recognised parameters of cell viability: namely, intracellular esterase activity and plasma membrane integrity. Probes such as fluorescein diacetate and its derivatives, which stain living cells, are non-polar molecules that readily pass through the cell membrane and enter the cytoplasm. Here, cytoplasmic esterases cleave acetate groups from the molecule, producing a polarised conjugated ring structure, which fluoresces green when excited with 488 nm blue light (Bell et al., 1988). Conversely, probes such as ethidium bromide and its derivatives will only enter the cell when the functional integrity of the membrane has been compromised. These probes bind exclusively to the dead cell nucleus, which appears red when photo-excited with 488 nm blue light (Lepecq and Paoletti, 1967).

More recently, a new generation of viability fluoroprobes has been introduced: live cell probes such as calcien-AM in combination with dead cell probes such as ethidium homodimer have greatly improved characteristics when compared to the early generation dyes (Moore et al., 1990). We report the use of these newer fluorescent viability probes primarily to visualise the living keratocyte network.

MATERIALS AND METHODS

Tissue samples

Complete globes were enucleated from 2- to 3-month-old pigs and 6- to 8-month-old steers obtained from the Auckland City Abbatoir 1-3 hours after slaughter.

For these initial studies, human corneæ found unsuitable for surgical transplantation by current assessment criteria, were obtained from the New Zealand National Eye Bank. Thus the human tissue examined was in a sub-optimal condition.

Dissection and storage of corneæ

Established sterile techniques were used to excise corneæ and a 3-5mm margin of scleral rim from the globes (Casey and Mayer, 1984). To maintain the corneo-scleral buttons in optimal condition, they were transferred to Corneal Organ Culture medium (Armitage and Moss, 1990), and maintained for periods of 2-24 hours at 34°C before further dissection and staining.

Preparation of corneæ for staining

The tissue sampling methods used in this study are illustrated in Fig. 1, and were specifically developed for use with the short working distance lenses available on the Leitz Dialux 20 microscope. Each corneo-scleral button was placed endothelial-side up in a drop of Corneal Organ Culture medium, and a strip 1-2 mm wide excised from across the entire central region of the cornea (Fig. 1A). The peripheral segments of this strip were removed (Fig. 1B), leaving a 5 mm × 2 mm strip of almost flat tissue from the centre of the cornea. This experimental sample was then dissected in one of two planes (Fig. 1).

Horizontal dissections

Routinely, three consecutive horizontal incisions were made in planes approximately parallel with the collagen lamellæ, to produce anterior, middle and posterior blocks (Fig. 1C). These 300-500 μm thick dissections included numerous undisturbed collagen lamellæ and keratocytes, which could be optically dissected by focussing through the depth of the sample. Thus, only keratocytes or collagen lamellæ falling within the depth of field of the lens (approximately 0.6 μm for the 25× phase/fluorescent objective used), were clearly imaged. Labelled keratocytes above or below the focal plane appeared as bright smudges in the field.

Antero-posterior dissections

Some antero-posterior dissections were made by cutting a series of slivers, approximately 500 μm thick by 2 mm wide, through the full antero-posterior thickness of the cornea (Fig. 1C). When mounted flat and viewed from the side, these dissections illustrated the spatial relationships between the epithelium, the stroma and the endothelium.

In both section planes the relatively sparse distribution of keratocyte fluorescence within the stroma was masked by the intense fluorescence within the dense cell populations of the live epithelium and endothelium. Consequently, the epithelial and endothelial cell layers were frequently removed to allow clear visualisation of the keratocyte subpopulations adjacent to Bowman's and Descemet's membranes.

Cytoplasmic staining

All fluoroprobes were obtained from Molecular Probes (Eugene, Oregon, USA), and were prepared and used according to the manufacturer's instructions. Dissections were placed in separate wells of a 24-well multiplate containing 0.25 ml of Live-Dead Assay,

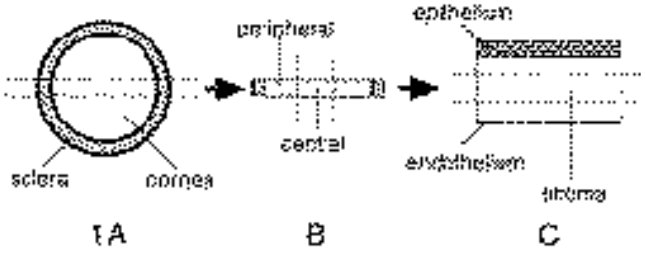

Fig. 1. Dissection of the corneæ prior to vital labelling and microscopic examination. (A) A strip of tissue was dissected from across the full width of the corneæ. (B) The central portion (10-15 mm^2) of the strip was selected, and dissected in the plane of the tissue, into three sections (C): anterior, central and posterior stroma. In most experiments, the epithelium and endothelium were removed.

which consists of a mixture of 2 μM of the vital dye calcein-AM, and 4 μM of the nuclear stain ethidium homodimer, in D-PBS (Dulbecco's phosphate buffered saline). These were stained in the dark at room temperature without agitation for 40 minutes and examined microscopically without subsequent washing.

Microscopy

All tissue dissections were carefully mounted on a slide in a drop of D-PBS, gently coverslipped, and excess moisture was removed to secure the sample flat. Dissections prepared in this manner were viewed using a Leitz Dialux 20 microscope fitted with a 25× phase-fluorescent, oil-immersion objective, and epi-illuminated with a 50 W mercury vapour lamp using a conventional (488 nm) fluorescein filter set. Photomicrographs were obtained using Ektachrome 400 colour transparency film, or TMAX-400 black and white film (Eastman Kodak Co., Rochester, N.Y., U.S.A.). Complementary phase-contrast micrographs were taken to view keratocytes in a single plane against the background of collagen lamellæ.

RESULTS

Corneal tissue

In these experiments, 2 bovine, 10 porcine and 4 human corneæ were examined, but comparative morphometric analysis was not performed as part of this study. Qualitatively, there appeared no significant differences in keratocyte morphology between these species and all fluoroprobes used gave identical patterns of staining. Due to their size and lack of inherent stiffness, bovine corneæ proved difficult to handle without risk of damage, and were included for comparative assessment only. On the other hand, porcine cornea were similar in size, stiffness and anatomy to the human corneæ, and were easily manipulated during dissection (Fig. 1). For these reasons the porcine cornea was principally used for the development of the labelling techniques.

Anterior stroma

This dissection contained the intensely fluorescent epithelium, Bowman's membrane, which was devoid of fluorescence, a highly cellular keratocyte layer directly beneath that membrane, and the anterior portion of the stroma proper (Fig. 2A).

The most significant feature of these dissections was the identification of a dense network of keratocytes, approximately 100 μm thick (the posterior boundary is indeterminate), directly posterior to the cell free Bowman's membrane (Fig. 2B). The keratocyte cell bodies in this layer showed lower levels of intracellular esterase activity than typical stromal keratocytes (see below) and appeared filamentous, elongate and often irregularly shaped (Fig. 2C). The remarkably diffuse and numerous cell processes tapering laterally from the cell bodies were thickest at their base, and frequently branched before making terminal contact with adjacent keratocyte processes. In antero-posterior dissections, no clear lamellar arrangement of the cells in this sub-Bowman's region was observed (Fig. 2A,B). Nerve fibres commonly found in this region also exhibited esterase activity, but were morphologically distinct from the keratocytes (Fig. 2C).

Posterior to this layer, the anterior portion of the stroma proper contained keratocytes with a morphology and distribution identical to those seen in central stromal dissections.

Central stroma

All vital fluoroprobes revealed an intensely and uniformly stained network of keratocytes within any single focal

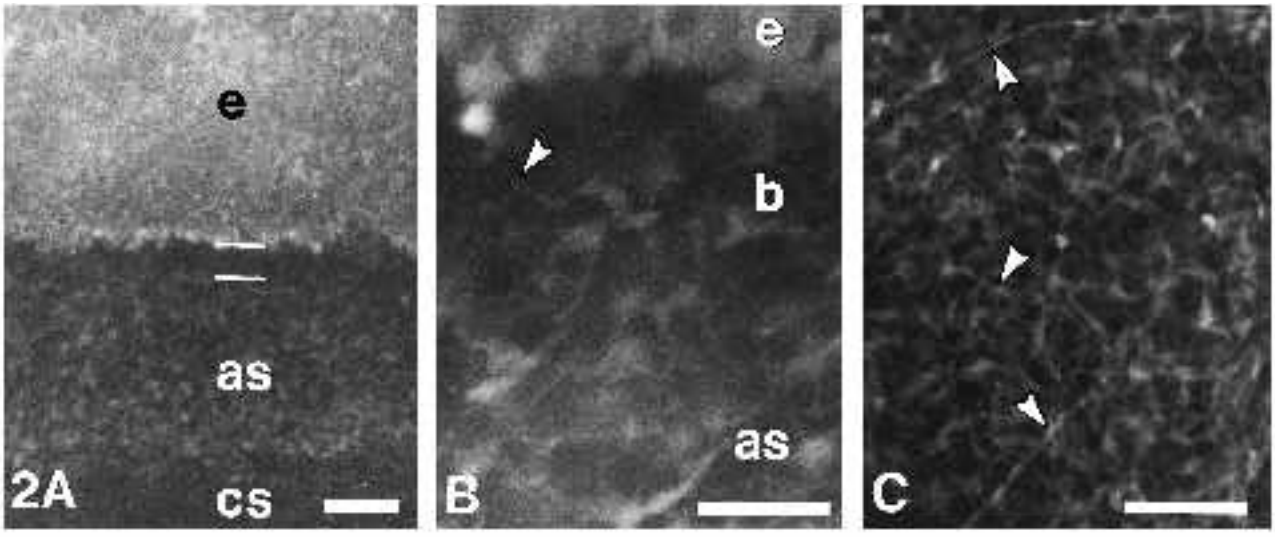

Fig. 2. Porcine cornea maintained overnight in organ culture medium and labelled with Live-Dead Assay. (A) Low-power antero-posterior plan through epithelium (e), Bowman's membrane (parallel lines), the dense cell layer forming the anterior stroma (as), and the anterior portion the central stroma (cs). Bar, 100 μm. (B) Detail of the interface between the epithelium (e) and the keratocytes of the anterior stroma (as). Note the general lack of cells in the region of Bowman's membrane (b), although some cell processes appear to traverse the apparent space to contact an epithelial cell (arrowhead). Bar, 50 μm. (C) Increased detail (lamellar dissection) showing the morphology and distribution of the keratocyte population in the anterior stroma. Fine nerve fibres labelled with calcien-AM were frequently observed in this layer (arrowheads). Bar, 100 μm.

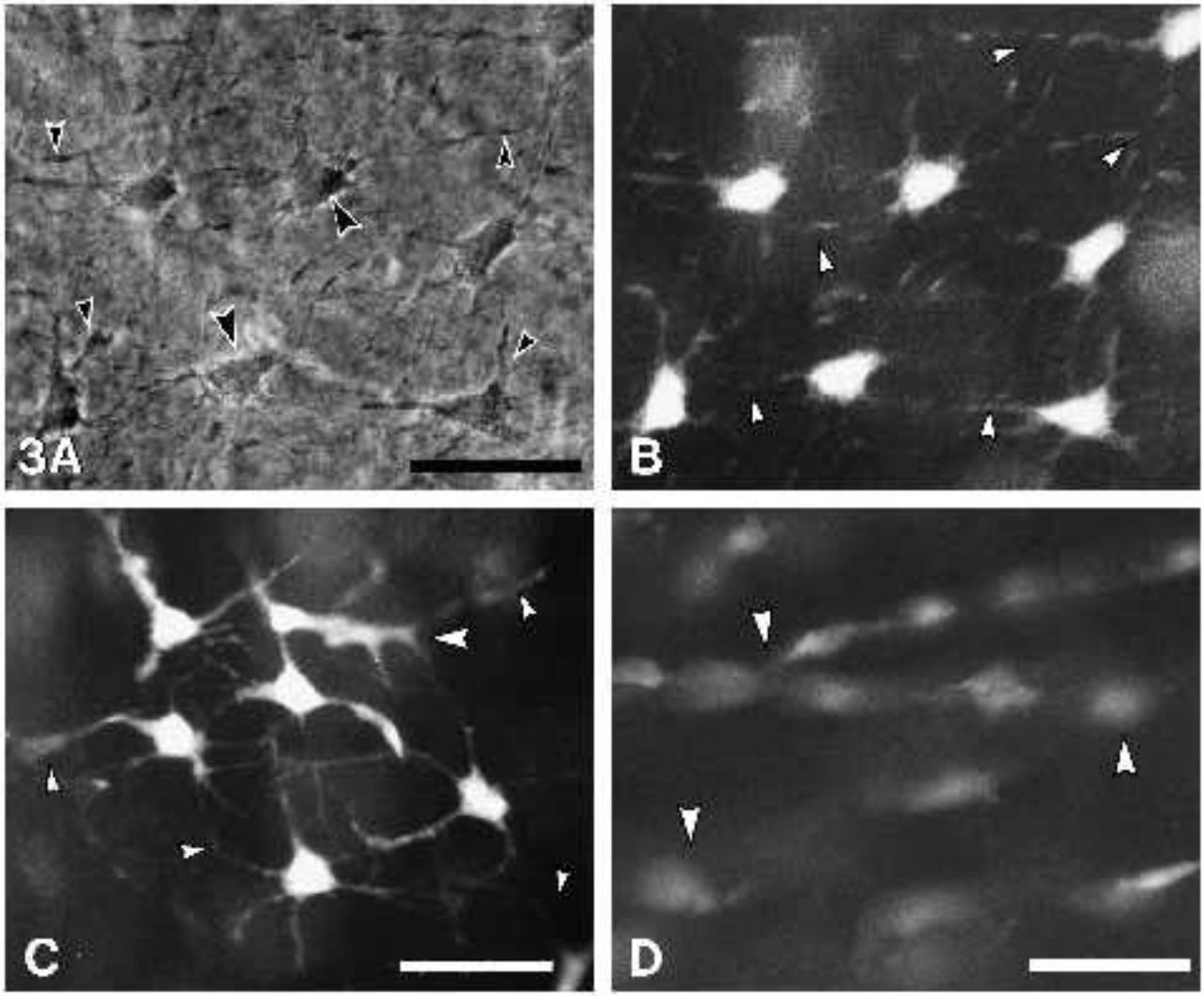

Fig. 3. Keratocytes in the central stroma. (A) Phase-contrast detail from a lamellar dissection of bovine cornea labelled with fluorescein diacetate and ethidium bromide. The keratocytes (large arrowheads) and their cell processes (small arrowheads) exhibit an orthogonal network arrangement. Bar, 50 μm. (B) Fluorescent image of the orthogonal network shown in A. Both keratocyte cell bodies and fine cell processes fluoresce brightly, indicating cells in the network are viable and make numerous contacts with adjacent cell processes (arrowheads). Fluorescent cell bodies of viable keratocytes below the focal plane appear as bright smudges (scale as for A). (C) Keratocyte organisation in the central stroma of porcine cornea labelled with Live-Dead Assay. Viable keratocyte cell bodies and cell processes in the plane of focus form a random network of interconnected cells. One keratocyte (large arrowhead) and several cell processes (small arrowheads) seem to project out of the focal plane. This suggests that keratocyte sheets are not strictly planar, but may have some degree of antero-posterior connection. Bar, 50 μm. (D) Detail of an antero-posterior dissection showing viable keratocytes in zig-zag sheets between interleaving stromal lamallæ. Ramping connections between alternating layers of keratocytes (arrowheads). Bar, 50 μm.

plane. These were organised in a range of patterns between adjacent collagen lamellæ, from a nearly orthogonal grid through to a near-random network (Fig. 3A,B,C). The orthogonal keratocyte network was seen in many but not all dissections viewed, suggesting this pattern was not a general feature of the mid-stromal keratocyte network as might have been anticipated from the work of Hogan et al. (1971). However, horizontal dissections inadvertently cut at a slight angle to the collagen lamellæ may also lead to apparent distortions in the keratocyte arrangement, and could contribute to inconsistencies in observations between preparations. This however, would only pertain to the cut surface and not deep within the dissection where optical sections are possible.

In the central stroma, the keratocyte cell bodies had a well-defined pyramidal or stellate shape with long, fine and generally unbranched cell processes projecting from their apices (Fig. 3B,C). Most frequently, these processes connected adjacent keratocytes within the same focal plane. Occasionally, however, they projected to keratocyte cell processes outside the plane of focus (Fig. 3C), suggesting some form of antero-posterior interlamellar connection between keratocytes in different planes.

Examination of antero-posterior dissections showed layers of keratocytes alternating with collagen lamellae (Fig. 3D). However, these layers of keratocytes were not always strictly parallel to each other; some were set at a slightly oblique angle to create a shallow ‘zig-zag’ pattern

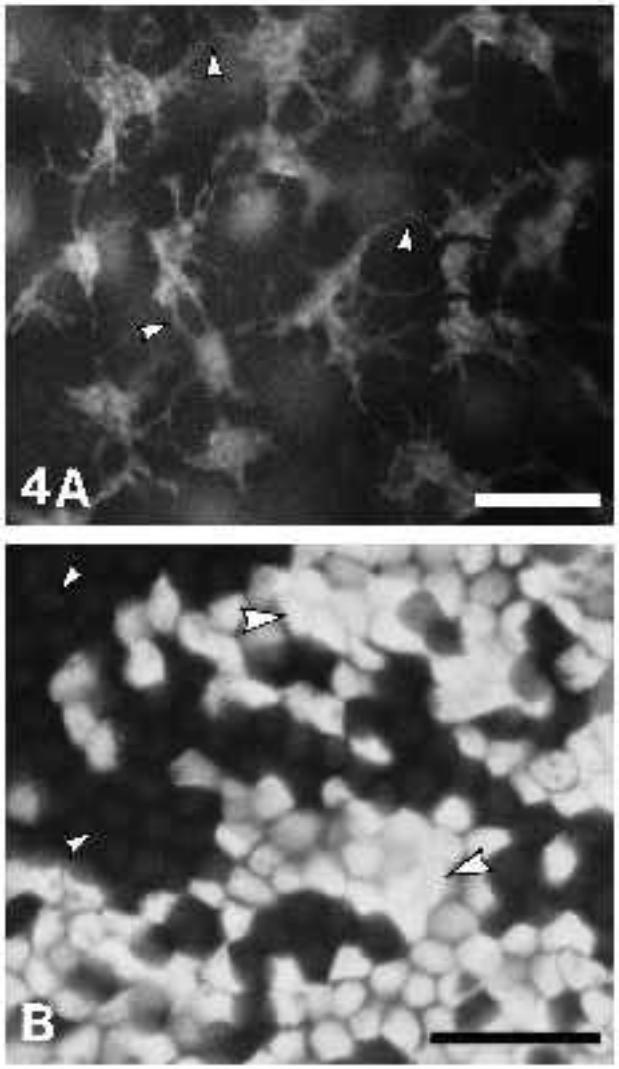

Fig. 4. Cells of the posterior stroma and endothelium labelled with fluorescein diacetate and ethidium bromide. (A) Porcine cornea showing detail of the viable keratocyte subpopulation that forms the layer immediately anterior to Descemet's membrane. Note the granular cytoplasm and the numerous connections between adjacent keratocytes (arrowheads). Bar, 50 μm. (B) Endothelium of human cornea stored in organ culture medium for 24 days, showing large areas of calcein-AM-labelled cells (large arrowheads) and patches of non-viable cells (small arrowheads), in which only the nuclei are stained with ethidium homodimer. Patches of dead endothelial cells are not uncommon in corneæ stored for extended periods as in this example. Bar, 50 μm.

of keratocytes through the antero-posterior depth of the stroma (Fig. 3D). These layers of keratocytes did not appear to transect one another, the terminal keratocytes of an oblique sheet intersecting with more horizontally oriented keratocyte groups to form a series of 'ramping connections' between alternating layers of keratocytes (Fig. 3D). Having identified these bridging cells, we are now developing refinements in experimental methods and imaging techniques to establish the nature and extent of these ramping connections, and their possible role in antero-posterior communication amongst stromal keratocytes.

Posterior stroma

Two distinct patterns of keratocyte staining were observed in posterior stromal dissections. The anterior part of these preparations had a keratocyte network identical in organisation and morphology to that found throughout the central stroma. Posteriorly, however, a morphologically distinct sub-population of keratocytes, two or three cell layers thick, was identified immediately anterior to Descemet's membrane (Fig. 4A). The endothelium defined the posterior boundary of these preparations and stained intensely (Fig. 4B).

The overall cell density of the narrow keratocyte population subjacent to Descemet's membrane was greater than that of the central stroma, while the esterase activity of these cells was reduced and had a granular, somewhat patchy distribution (Fig. 4A). The cell bodies of these keratocytes were significantly larger and more irregular in shape than mid-stromal keratocytes, with a greater number of lateral cell processes. These processes were generally shorter and thicker, and branched more than typical stromal keratocytes, with several processes forming an irregular network connecting many of the cells within a narrow focal plane. This distinct layer of keratocytes could also be seen in antero-posterior dissections, but there was no evidence of labelled cells or fine cell processes passing into or through the cell-free Descemet's membrane.

DISCUSSION

The use of fluorescent markers to trace dynamic intracellular reactions has expanded rapidly in recent years, due largely to the continued development, production and availability of site-specific, fluorescently labelled lectins. During initial trials on intact fragments of articular cartilage, fluorescein diacetate used as an intracellular marker of esterase activity gave a consistent fluorescent distribution throughout the cytoplasm of the chondrocytes (Poole et al., 1991). We concluded that, in addition to providing evidence of cell viability, fluorescein diacetate and its derivatives also had the capacity to 'trace' the distribution of the cytoplasm and allowed a clear definition of viable cell morphology within an unstained extracellular matrix.

This study utilised whole-mount samples of intact living corneæ and viability probes to examine the detailed morphology, distribution and organisation of living keratocytes in the intact corneal stroma. Simple sampling and limited dissection techniques have been used to create thick (300-500 μm) whole mounts of untreated, freshly collected corneæ. These samples were completely transparent and did not suffer the typical tissue distortion and opaqueness introduced by aldehyde fixation or cryopreservation in previous studies of keratocyte morphology and ultrastructure. The optical transparency and transmittance from within the sample enabled light microscopic examination through considerable depth of dissected cornea. Consequently, this study is unique in showing the distribution and organisation of living keratocytes within the three-dimensional structure of corneal samples that have suffered a minimum amount of physical or chemical distortion.

In initial experiments we tried the earlier generation vital dyes fluorescein diacetate or 5,6-carboxyfluorescein diacetate used in combination with the dead cell probe ethidium bromide. Whilst these dyes adequately demonstrated keratocyte viability or morbidity, three key problems were encountered during their use. Firstly, failure to wash the tissue dissections properly before viewing resulted in unacceptable background fluorescence in the extracellular matrix, while excessive washing was thought to contribute to the high rate of cell death observed in some preparations. Second, these fluoroprobes were particularly susceptible to fluorescent quenching during examination. To overcome this problem, the anti-fading agent CitiFluor (Agar EM, UK) was added immediately before viewing and, although it did retard quenching of the fluorescence, it proved to be cytotoxic. Finally, these fluoroprobes were pH-sensitive with a visible shift in the emission spectrum of fluorescein diacetate from green to yellow as the intracellular pH decreased during keratocyte death.

Given these difficulties, the new generation assay, Live-Dead Assay, a combination of calcien-AM and ethidium homodimer was evaluated. When compared with the early generation fluoroprobes, Live-Dead Assay exhibited greatly improved characteristics: its chemical stability, high retention rate within cells, low background fluorescence, and high resistance to fluorescent quenching. Moreover, these preparations required no special incubation or washing before examination (Moore et al., 1990), which reduced artefacts and revealed the delicate keratocyte network alive and intact. These fluoroprobes also proved to be pH-insensitive, maintained a uniform emission spectrum during the period of examination and showed a consistent and reliable staining pattern. To our knowledge these relatively simple histochemical techniques have not previously been used to study the keratocyte, an application to which they appeared uniquely suited in that the tissue's inherent transparency was utilised to image the undisturbed cell within the three-dimensional stromal matrix.

Esterase enzymes are ubiquitously distributed throughout the cytoplasm of most viable cells and are able to cleave the non-polar probes that penetrate intact cell membranes, releasing fluorescently activated molecules within the cytoplasm. Consequently, even the cytoplasm of small cell processes fluoresce when activated by 488 nm blue light. The improved sensitivity and resolution of the fluoroprobe techniques used here when compared with previous histological methods for examining this tissue (Hogan et al., 1971; Nishida et al., 1988) revealed an extremely complex network of very fine interconnecting cell processes, which seemed to typify keratocyte morphology seen within our preparations.

Two key factors contributed to the success of this approach: the penetrability of the dyes and their physicochemical characteristics; and the transmittance of the fluorescing cells within a non-fluorescing, transparent matrix. These characteristics, coupled with tissue dissections in well-defined anatomical planes, have not only enabled us to see the organisation of the keratocytes, but also to begin to place them more precisely within the context of the three-dimensional collagenous matrix that dominates the stroma. Concepts of the nature, structure and organisation of stromal collagen lamellæ are being reviewed as more becomes known of its biochemistry. It is also suspected that the arrangement of the collagen fibrils may be more complex (Komai and Ushiki, 1991) than implied in the previously described lamellar lattice structure (Hogan et al., 1971). Should the orientation of the collagen fibrils not be consistently parallel, this would permit the more random disposition of keratocytes that were present in some of our mid-stromal preparations, and in the regions subjacent to Bowman's and Descemet's membranes.

This study identifies three morphologically distinct keratocyte subpopulations, two of which have not been clearly identified before and were located in transitional zones abutting onto, and at the extreme edge of, the definitive stroma where collagen fibrils differ in arrangement and diameter. The first was identified as a dense cell layer, approximately 100 μm thick, immediately posterior to Bowman's membrane in the anterior stroma. A second narrower layer (1-2 cells thick), was found in the posterior stroma immediately subjacent to Descemet's membrane. These two sub-populations represented only a small proportion of the total keratocyte population.

The morphology of the keratocytes posterior to Bowman's and anterior to Descemet's membrane's differed significantly from typical stromal keratocytes, yet they shared certain features in common. Both had a granular appearance, displayed lower levels of intracellular esterase activity, and formed extensive cytoplasmic cell processes that frequently branched to produce a fine fenestrated network. However, keratocytes posterior to Bowman's membrane had smaller cell bodies than those found anterior to Descemet's membrane.

Previous studies have shown little evidence of morphologically distinct keratocyte subpopulations in different regions of the stroma. Early silver staining studies by Scharenberg (1955) showed 'shadowy polymorph elements' in the anterior stroma of the human cornea, which appear to have a morphology similar to that reported here using esterase fluoroprobes. More recent studies by Stockwell (1991) have also shown that the human keratocyte nucleus, in proportion to the total cell volume, decreases in size as the distance from the epithelium increases, while sub-epithelial keratocytes in sheep and humans were also shown to have a larger mitochondrial volume density than elsewhere in the stroma. Differences in the lectin binding properties of keratocytes in the posterior stroma have also been reported (Schanzlin et al., 1990), but no correlations were made with keratocyte morphology. Thus, whilst this study identified morphologically distinct subpopulations of keratocytes restricted to narrow segments of stroma subjacent to the epithelium and endothelium, the extent and distribution of these keratocytes, their precise relationships to Bowman's and Descemet's membranes and the recognition of any specific functions performed by them have yet to be determined.

The third and most common keratocyte population was distributed throughout the bulk of the stromal volume and formed the majority of cells studied. These cells were characterised by flattened, triangulate cell bodies and clearly defined cell processes. In all species examined, a spectrum of keratocyte arrangements was observed within one focal

plane, from precise orthogonal grids to more random cellular arrays (Fig. 3A,B,C). These observations correlate with previous descriptions of keratocyte morphology and are to a large extent consistent with the view that keratocytes form flat, interlamellar sheets (Hogan et al., 1971; Marshall and Grindle, 1978). Neighbouring cell bodies had a profuse network of laterally oriented and interconnecting processes within a single focal plane. However, some of these processes did curve out of focus, suggesting the presence of antero-posterior connections between keratocytes above or below the optical plane of section. Antero-posterior dissections also revealed intersecting sheets of keratocytes that formed oblique cellular 'ramps' zig-zagging through the antero-posterior axis of the stroma. Of particular interest is the suggestion that some form of antero-posterior connections could represent the anatomical correlate of a functional, three-dimensional keratocyte intercellular communication network. Whilst it is possible that these obliquely placed sheets of keratocytes may provide some form of 'ramping connection' between adjacent lamellæ, further studies are required to accurately identify functional antero-posterior connections within the keratocyte network.

In summary, we report that fluorescently labelled viable keratocytes are strongly contrasted against unlabelled collagen lamellae, allowing the visualisation of these cells within the three-dimensional stroma. Secondly, the distribution of esterase-sensitive viability dyes throughout the cytoplasm of the keratocytes enabled the detailed morphology and arrangement of the living keratocyte network to be investigated. Finally, we found variations in cellular morphology, identified cell subtypes, and were able to trace the course and spatial orientation of connecting cell processes within the corneal stroma. The application of this investigatory histochemical technique within our laboratory to circumstances in which the keratocyte and its environment are challenged or changed, shows promise of providing a unique and significant new approach to achieving a better understanding of the microanatomy and dynamic interactions of keratocytes within the corneal stroma.

We thank Professor Phillippa Wiggins for her helpful comments on this manuscript.

REFERENCES

Armitage, W. J. and Moss, S. J. (1990). Storage of corneas for transplantation. In *Current Ophthalmic Surgery* (ed. D. L. Easty), pp. 193-199. London: Baillère Tindal.

Assouline, M., Chew, S. J., Thompson, H. W. and Beuerman, R. (1992). Effect of growth factors on collagen lattice contraction by human keratocytes. *Invest. Ophthalmol. Vis. Sci.* **33**: 1742-1755.

Bell, R. S., Bouret, L. A., Bell, D. F., Gebhardt, M. C., Rosenberg, A., Treadwell, B. V., Tomford, W. W. and Mankin, H. J. (1988). Evaluation of fluorescein diacetate for flow cytometric determination of cell viability in orthopædic research. *J. Orthop. Res.* **6**, 467-474.

Birk, D. E., Fitch, J. M., Babiarz, Doane, K. J. and Linsenmayer, T. F. (1990). Collagen fibrillogenesis *in vitro*: interaction of types I and V collagen regulates fibril diameter. *J. Cell Sci.* **95**, 649-657.

Birk, D. E., Lande, M. A. and Fernandez-Madrid, F. R. (1981). Collagen and glycosaminoglycan synthesis in aging human keratocyte cultures. *Exp. Eye Res.* **32**, 331-339.

Casey, T. A. and Mayer, D. J. (1984). *Corneal Grafting.* W. B. Saunders, London.

Cintron, C. and Hong, B.-S. (1988). Heterogeneity of collagens in rabbit cornea: type VI collagen. *Invest. Ophthalmol. Vis. Sci.* **29**, 760-766.

Hogan, M. J., Alvarado, J. A. and Weddell, J. E. (1971). *Histology of the Human Eye.* Saunders. Philadelphia.

Kohno, T., Sorgente, N., Ishibashi, T., Goodnight, R. and Ryan, S. J. (1987). Immunofluorescent studies of fibronectin and laminin in the human eye. *Invest. Ophthalmol. Vis. Sci.* **28**, 506-514.

Komai, Y. and Ushiki, T. (1991). The three-dimensional organization of collagen fibrils in the human cornea and sclera. *Invest. Ophthalmol. Vis. Sci.* **32**, 2244-2258.

Lepecq, J. F. and Paoletti, C. (1967). A fluorescent complex between ethidium bromide and nucleic acids. Physical-chemical characterisation. *J. Mol. Biol.* **27**, 87-106.

Marshall, J. and Grindle, C. F. J. (1978). Fine structure of the cornea and its development. *Trans. Ophthalmol. Soc.* **98**, 320-328.

Maurice, D. M. (1957). The structure and transparency of the cornea. *J. Physiol.* **136**, 263-286.

Maurice, D. M. (1984). The cornea and sclera. In *The Eye*, vol. 1B (ed. H. Davson), pp. 1-158. New York, London: Academic Press.

Moore, P. L., MacCoubrey, I. C. and Haugland, R. P. (1990). A rapid, pH insensitive, two colour fluorescence viability (cytotoxicity) assay. *J. Cell Biol.* **111**, 58.

Nishida, T., Yasumoto, K., Otori, T. and Desaki, J. (1988). The network structure of corneal fibroblasts in the rat as revealed by scanning electron microscopy. *Invest. Ophthalmol. Vis. Sci.* **29**, 1887-1890.

Poole, C. A., Matsuoka, A. and Schofield, J. R. (1991). Chondrons from articular cartilage. III. Morphologic changes in the cellular microenvironment of chondrons isolated from osteoarthritic cartilage. *Arthritis Rheum.* **34**, 22-35.

Schanzlin, D. J., Kratz-Owens, K. and Hageman, G. S. (1990). Keratocyte subpopulation as revealed by lectin-binding. *Invest. Ophthalmol. Vis. Sci.* **31; Suppl.,** 32.

Scharenberg, K. (1955). The cells and nerves of the human cornea. *Amer. J. Ophthal.* **40**, 368-279.

Schittny, J. C., Timpl, R. and Engel, J. (1988). High resolution immunoelectron microscopic localisation of functional domains of laminin, nidogen, and heparan sulphate proteoglycan in epithelial basement membrane of mouse cornea reveals different topological orientations. *J. Cell Biol.* **107**, 1599-1610.

Smith, J. W., Christie, K. N. and Frame, J. (1969). Desmosomes, cilia and acanthosomes associated with keratocytes. *J. Anat.* **105**, 383-392.

Stockwell, R. A. (1991). Morphometry of cytoplasmic components of mammalian articular chondrocytes and corneal keratocytes: species and zonal variations of mitochondria in relation to nutrition. *J. Anat.* **175**, 251-261.

Sverdlick, J. (1954). Study of keratocytes by means of del Rio Hortega's method of silver impregnation. *Acta XVII int. Cong. Ophthal.* **3**, 1887.

Toynbee. (1841). *Philos. Trans.* **131**, 159. As quoted by Duke-Elder, S. and Wybar, K. C. (1961). *System of Ophthalmology*, vol. 3 (ed. S. Duke-Elder), pp. 107. London: Henry Kimpton.

Ueda, A., Nishida, T., Otori, T. and Fujita, H. (1987). Electron-microscopic studies on the presence of gap junctions between corneal fibroblasts in rabbits. *Cell Tiss. Res.* **249**, 473-475.

(Received 14 April 1993 - Accepted, in revised form, 21 July 1993)